Available online at www.sciencedirect.com
SCIENCE DIRECT
Marine Micropaleontology 59 (2006) 15–34
MARINE MICROPALEONTOLOGY
www.elsevier.com/locate/marmicro

Coccolithus pelagicus subsp. *pelagicus* versus *Coccolithus pelagicus* subsp. *braarudii* (Coccolithophore, Haptophyta): A proxy for surface subarctic Atlantic waters off Iberia during the last 200 kyr

Aurea Narciso [a,*], Mario Cachão [b], Lucia de Abreu [c,d]

[a] *PhD scholarship SFRH/BD/8944/2002; Centre Geology University of Lisbon, Building C6, 6.4.67, Campo Grande, 1749-016 Lisboa, Portugal*
[b] *Centre Geology University of Lisbon and Department of Geology, Fac. Sciences, University of Lisbon, Building C6, 6.4.55, Campo Grande, 1749-016 Lisboa, Portugal*
[c] *Godwin Laboratory, University of Cambridge, Pembroke Street, New Museums Site, Cambridge CB2 3SA, United Kingdom*
[d] *INETI, Department of Marine Geology, Estrada da Portela, Zambujal, 2720 Alfragide, Portugal*

Received 21 July 2005; received in revised form 2 December 2005; accepted 15 December 2005

Abstract

A Multivariate Morphon Analysis (MMA) of *Coccolithus pelagicus* (s. l.) coccoliths was performed on 178 samples from an oceanic core recovered off the Portuguese margin (MD95-2040), in order to define the morphometric boundaries of its morphotypes and their behaviour during the last two glacial cycles. The recurrent occurrence of the smaller morphotype of this taxon, *C. pelagicus* subsp. *pelagicus*, was recognized for the first time off the Portuguese coast. Three sections, around Heinrich Layers 1 and 6 and Termination II-Eemian, were selected to establish high resolution comparisons between *C. pelagicus* subsp. *pelagicus* and *C. pelagicus* subsp. *braarudii* and two independent proxies for cold water masses: the records of the planktonic foraminifera *Neogloboquadrina pachyderma* (sinistral) and ice-rafted detritus (IRD). There is an overall negative correlation between *C. pelagicus* subsp. *pelagicus* and *C. pelagicus* subsp. *braarudii* as expressed by MMA Factor 1, the scores of which respond similarly to those of two non-coccolithophore proxies and consequently, is proposed as a calcareous nannoplankton proxy for the influence of subpolar waters in the region. Detailed analysis, however, showed occasional decoupling amongst these three proxies, which are used to highlight significant changes between the cooling–warming sequences of distinct events off Iberia.

Keywords: Palaeoceanography; palaeoecology; Heinrich Layer; Western Iberia; *Coccolithus pelagicus* (s. l.); *C. pelagicus* subsp. *pelagicus*; *C. pelagicus* subsp. *braarudii*

1. Introduction

Coccolith morphometry has already been used to address questions such as taxonomy, biostratigraphy and palaeoecology of several calcareous nannoplankton (e.g. Samtleben, 1980; Backman and Hermelin, 1986; Young, 1990; Wei, 1992; Baumann, 1995; Knappertsbusch, 2000; Colmenero-Hidalgo et al., 2002). This approach is based on the fact that heterococcoliths (hereafter simply referred to as coccoliths), being produced intracellularly, are completed formed prior to being extruded from the coccosphere (e.g. Westbroek et al., 1984, Young et al., 1999; Young and Henriksen, 2003), hence their dimensions may be

* Corresponding author. Fax: +351 217500119.
E-mail addresses: acnarciso@fc.ul.pt (A. Narciso), mcachao@fc.ul.pt (M. Cachão), 1d206@cus.cam.ac.uk (L. de Abreu).

0377-8398/$ - see front matter © 2005 Elsevier B.V. All rights reserved.
doi:10.1016/j.marmicro.2005.12.001

considered to be an intrinsic property of a particular species or ecophenotype.

Coccolithus pelagicus (s. l.) has been one of the most commonly and easily interpreted calcareous nannofossil species, being used as a proxy for cold waters (McIntyre and Bé, 1967; Okada and McIntyre, 1979; Winter et al., 1994; Baumann, 1995; Andruleit, 1997). However, studies performed off Iberia showed that the biogeography of *C. pelagicus* (s. l.) also included upwelling regions (Cachão and Moita, 2000). This apparent contradiction started to be resolved when Geisen et al. (2002) presented life cycle evidences for the existence of two extant subspecies of *C. pelagicus*: *C. pelagicus* subsp. *pelagicus*, the subarctic form, and *C. pelagicus* subsp. *braarudii*, the temperate form, related to moderate fronts, namely those driven by upwelling conditions (Cachão and Moita, 2000). In 2003, Sáez et al. concluded that there were also genetic differences between these two entities (Sáez et al., 2003). Important for micropalaeontological studies, these subspecies can also be recognized by the size of their placoliths (Baumann, 1995), the former being smaller (7–10 μm) and the latter larger (10–16 μm) (Geisen et al., 2002; Parente et al., 2004). More recently, based on detailed morphometric analysis, Parente et al. (2004) confirmed the existence of three morphotypes of *C. pelagicus* (s. l.): the smaller morphotype related to *C. pelagicus* subsp. *pelagicus*, the intermediate size morphotype related to *C. pelagicus* subsp. *braarudii*, and a larger new one described as *C. pelagicus* subsp. *azorinus* (see Jordan et al., 2004). In this work, this taxonomic subdivision will be adopted.

Several authors showed already that the Polar Front position changed through time, playing an important role in the Iberian palaeoclimate (e.g. Fatela, 1995; Zazo et al., 1996). For instance, during the last glaciation, Ruddiman and McIntyre (1981) suggested that maximum southward advance of the Polar Front reached 42°N, whereas the studies of Duprat (1983) established a limit of 38°N for the same period. Later, Bard et al. (1987) concluded that during the earliest retreat of the last glaciation, the Polar Front moved from 35°N to 55°N. In contrast, Fatela et al. (1994) showed that during the last glaciation the Polar Front did not migrate south of 42°N.

The present work will discuss the influence of the migration of the polar system closer to Iberia through the presence of *C. pelagicus* subsp. *pelagicus*, the subarctic species, during the two last glacial cycles, and to compare its (factorial scores) record with the records of the two well known independent proxies for cold water masses: planktonic foraminifera *Neogloboquadrina pachyderma* (sinistral variety) and ice-rafted detritus (IRD) during selected time intervals. The selected intervals correspond to the Heinrich Layers 1 and 6 and Termination II-Eemian when placoliths of *C. pelagicus* (s. l.) are particularly abundant and with distinct patterns.

2. Core location and oceanographic setting

This study was based on core MD95-2040, recovered in July 1995 east of the Oporto Seamount off the Portuguese margin (latitude 40°34.91′ N, longitude 09°51.67′ W) (Fig. 1) (Bassinot et al., 1996).

The studied sector is a hydrodynamically active area, where water masses of different sources and properties converge and interact, following a dynamic vertically layered pattern, established as a function of temperature, salinity and dissolved oxygen content (de Abreu, 2000). This core provides a continuous pelagic record apparently unaffected by winnowing or significant chemical dissolution (de Abreu, 2000). In this eastern part of the North Atlantic subtropical gyre, the properties of modern surface water are influenced by the descending branch of the North Atlantic Drift (Portugal Current) and by a seasonal upwelling regime during summer months. This upwelling system is associated with the increase in the intensity and steadiness of northerly winds (Portuguese Trade Winds), as a consequence of the Azores anticyclone intensification and its westward movement during summer (Fiúza et al., 1998). In the northeastern border of the subtropical gyre, acting as a continuous link to the south-eastern

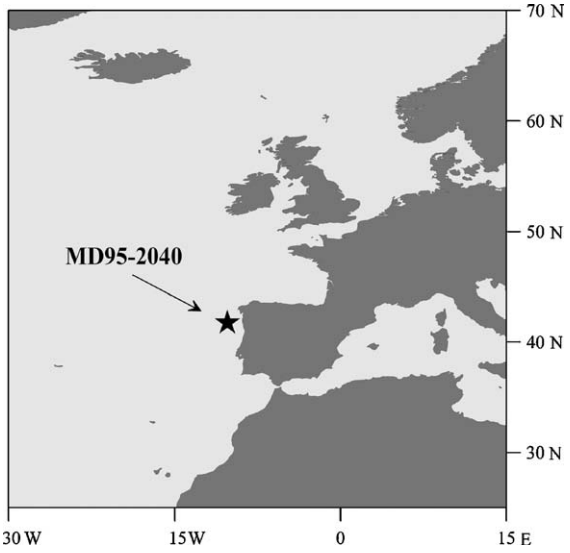

Fig. 1. Location of the core MD95-2040.

branch of Gulf Stream, flows the Azores Current (Klein and Siedler, 1989). South of the Azores Islands the Azores Current coincides with the Azores Front, which is characterized by a zone of strong hydrographic transition, in terms of temperature (Gould, 1985) and water column structure (Fasham et al., 1985). Towards the East Atlantic margin, the geographic positions of these two entities are separated; the Azores Current continuing eastwards to the Strait of Gibraltar, while the Azores Front degenerates into two weaker transitions, one lying to the west of the Gulf of Cadiz and another lying further to the south flowing between the Canary Islands and North Africa (Johnson and Stevens, 2000). The region is also influenced by the North Atlantic Oscillation (NAO) in such a way that low NAO indices are related to higher atmospheric moisture in Western Iberia, coeval with warm temperatures over Greenland, while high NAO values are associated with Iberian aridity and cold temperatures over Greenland (Hurrel, 1995; Rodó et al., 1997).

3. Materials and methodology

MD95-2040 core, collected during the IMAGES MD101 cruise aboard the R/V *Marion Dufresne*, was recovered with a Calypso giant piston corer from a depth of 2465 metres below sea-level (mbsl), and is 35.24 m long (Bassinot et al., 1996).

A sample set of this core (178 samples) was used to analyse morphometric changes during marine isotope stages (MIS) 1 to 7 (de Abreu, 2000; de Abreu et al., 2003). Three sections with 58, 34 and 51 samples, corresponding to the Heinrich Layer 1 (HL1), Heinrich Layer 6 (HL6) and to the interval from Termination II to the Eemian (TII-E), respectively, were subsequently studied in detail due to the higher relative abundances of *C. pelagicus* subsp. *pelagicus*.

Smear slides were prepared and observed under an optical polarizing microscope (OLYMPUS BX-40), at a 1250× magnification, connected to a digital camera (OLYMPUS DP11). For morphometry, 100 placoliths were randomly selected throughout the slide of each sample, and their maximum diameters (length) measured (Fig. 2).

The image analysis program Scion-Image, equipped with a suite of routines (www.nhm.ac.uk/hosted_sites/ina/CODENET/Coccobiom) and adapted to PC, was used to: (1) group the images in mosaics, so that multiple coccolith images could be seen simultaneously; (2) measure the main axis of each coccolith; and (3) copy the results to a spreadsheet for subsequent statistical analysis. The morphometric parameters were directly

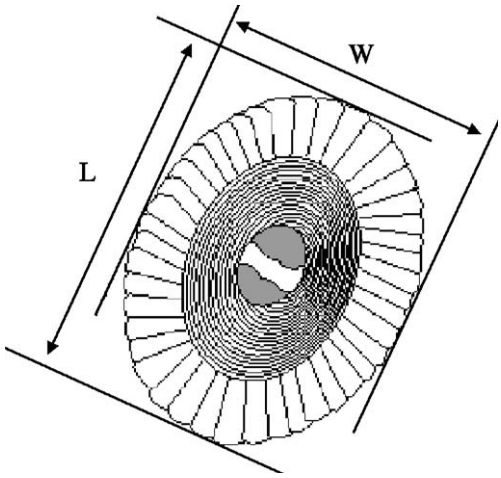

Fig. 2. Schematic distal view of a *C. pelagicus* coccolith and main morphometric parameters (L—length, W—width).

measured on frame-grabber captured digital images at magnifications of about 2500×. The measurement-associated error is ± 0.1 μm. For statistical analysis of the palaeoecological distributions specimens were assigned to 1 μm size integer intervals, hereafter referred to as morphons. For example, morphon 10 includes all specimens which have a maximum diameter within the interval [10.0, 11.0[μm.

A morphometric data matrix, with samples as rows and morphons as columns, was subjected to R-mode Factor Analysis. This analysis, herein referred to as Multivariate Morphon Analysis (MMA), tests which contiguous morphons show high positive correlation and thus define a specific morphotype. A factor may be characterized by a single morphotype, with a particular and distinguishable behaviour along the entire data set, or by the opposite behaviour between two distinct morphotypes. Based on the percentage of the variance (of the initial data matrix) that each factor represents, a factor is considered relevant or not. This procedure allows: (1) to statistically test the existence of distinct morphotypes in the data set; (2) to define their morphometric boundaries and how they may change; and (3) to analyse the relative behaviour of the morphotypes along the time series. All statistical data processing used the program STATISTICA® version 7.

The age model of the MD95-2040 core, established from a combination of oxygen isotope stratigraphy, ^{14}C dating and synchronisation of the sea-surface temperature (SST) records and the GISP2 $\delta^{18}O$ data, is discussed in de Abreu et al. (2003). Isotopic stages are recognized and ages assigned in accordance with the standard curve SPECMAP of Martinson et al. (1987). The detailed stratigraphy for the last deglaciation and

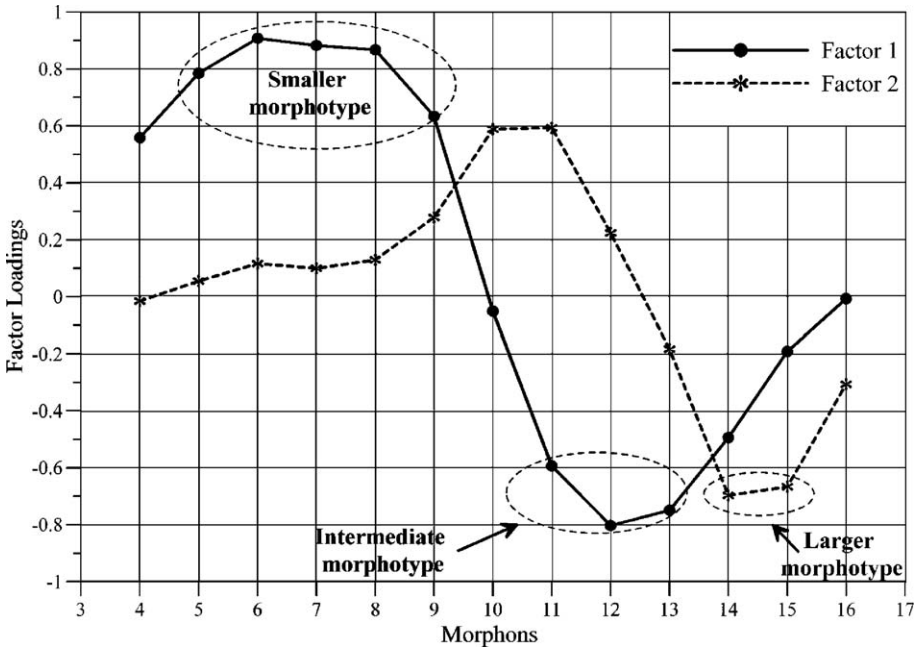

Fig. 3. F1 and F2 loadings for the several morphons observed in core MD95-2040 sample set (analysis performed on 98 samples). Extraction: Principal factors (comm.=multiple *R*-square) with varimax raw. Marked loadings are >|0.7|.

the Holocene is consistent with the planktonic $\delta^{18}O$ record from the nearby core SU81-18 (37°46′ N, 10°11′ W) described in Bard et al. (1989) (de Abreu, 2000; de Abreu et al., 2003).

The palaeotemperature estimates for MD95-2040 are from de Abreu (2000) and were obtained with both the CLIMAP transfer function equation FA20 (Imbrie and Kipp, 1971) and with a modern analogue technique SIMMAX 28 (Pflaumann et al., 1996).

4. Results

4.1. Multivariate Morphon Analysis (MMA)

4.1.1. Overall MD95-2040 core

Factor analysis performed on the overall morphometric data (MMA) of MD95-2040 (Appendix 1; http://correio.fc.ul.pt/~mcachao/papers/morphon/Appendix1.pdf) resulted in two factors, each related to a highly correlative combination of morphons, and which defines three morphotypes (Fig. 3, Table 1). Factor 1, with a variance of 43%, is strongly influenced by morphons 5 to 9 (5 to 8 with loadings higher than 0.7 and 9 with loadings of 0.63) in negative correlation to morphons 12 and 13 (with loadings higher than 0.7), reflecting an opposite behaviour between these two clusters of morphons, the two morphotypes associated to *C. pelagicus* subsp. *pelagicus* and *C. pelagicus* subsp. *braarudii*, respectively.

Factor 2, with a variance of 15%, is directly related to morphons 14 (with loadings of 0.7) and 15 (with loadings of 0.67), consequently describing the presence of a distinct and potentially meaningful larger morphotype with coccolith lengths longer than 14.0 μm.

The comparison of F1 scores against sea surface temperatures (warm and cold) shows a negative correlation between the smaller/intermediate morphotypes and the temperature of surface waters (Fig. 4a and b).

Table 1
Factor loadings for entire MD95-2040 core

Variable	Factor 1	Factor 2
Morphon 4	0.5584	−0.0156
Morphon 5	0.7853*	0.0549
Morphon 6	0.9076*	0.1163
Morphon 7	0.8823*	0.0995
Morphon 8	0.8672*	0.1294
Morphon 9	0.6334	0.2783
Morphon 10	−0.0508	0.5887
Morphon 11	−0.5935	0.5929
Morphon 12	−0.8028*	0.2238
Morphon 13	−0.7495*	−0.1832
Morphon 14	−0.4941	−0.6971*
Morphon 15	−0.1909	−0.6666
Morphon 16	−0.0073	−0.3064
Expl. var.	5.5257	1.9267
Prp. tot.	0.4251	0.1482

Extraction: Principal factors (comm.=multiple *R*-square) with varimax raw.
Marked loadings (*) are >|0.7|.

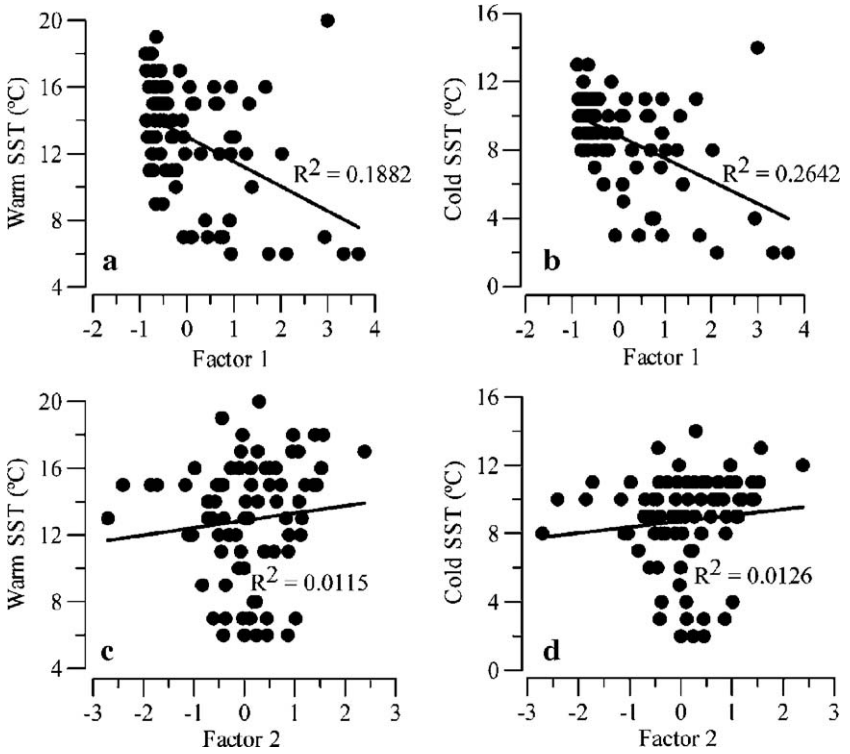

Fig. 4. Plot of F1 and F2 scores against cold and warm palaeotemperatures estimated by the SIMMAX 28 (de Abreu, 2000). a—Factor 1 vs warm SST; b—Factor 1 vs cold SST; c—Factor 2 vs warm SST; d—Factor 2 vs cold SST.

F2 scores, on the other hand, show no such correlation (Fig. 4c and d).

4.1.2. Heinrich Layer 1

MMA performed on the HL1 data matrix (Appendix 2; http://correio.fc.ul.pt/~mcachao/papers/morphon/Appendix2.pdf) shows there is just one factor for this time slice (Fig. 5, Table 2). This factor, with a variance of 63%, describes the behaviour of a small morphotype, characterized by morphons 4 to 9 (with loadings higher than 0.7), in perfect opposition to an intermediate one, characterized by morphons 11 to 14 (with loadings also higher than 0.7). Morphon 10 is characterized by almost null loadings thus defining the morphometric boundary between these two morphotypes (Fig. 5).

4.1.3. Heinrich Layer 6

MMA performed on the HL6 data matrix (Appendix 3; http://correio.fc.ul.pt/~mcachao/papers/morphon/Appendix3.pdf) shows that the specimens' behaviour is somehow more complex, needing two factors to describe it (Fig. 6, Table 3). Factor 1, with a variance of 50%, is strongly influenced by the opposite behaviour between morphons 5 to 9 (small morphotype) and 11 to 13 (intermediate morphotype), all with absolute loadings higher than 0.7. Again it depicts strong opposite behaviour between these two morphotypes. Factor 2, on the one hand, with a variance of 15%, explains the independent behaviour of the morphons 14 and 15 (the first one with loadings of $|-0.61|$ and the last one with loadings of $|-0.74|$), characterizing a large morphotype together with the occurrence of coccoliths, the lengths of which are in the limit between the small and the intermediate morphotypes (10 μm; with loadings of 0.79).

4.1.4. Termination II-Eemian

MMA performed on the TII-E data matrix (Appendix 4; http://correio.fc.ul.pt/~mcachao/papers/morphon/Appendix4.pdf) depicts the appearance of the three distinct morphotypes whose behaviour can also be explained through two factors (Fig. 7, Table 4). Factor 1, with a variance of 49%, describes again the opposite behaviour between the small and the intermediate morphotypes by disclosing important negative correlation between morphons 5 to 9 and morphons 11 to 13 (all with absolute loadings higher than 0.7). Factor 2, with a variance of 18%, is related to morphons 14 and 15 (with absolute loadings higher than 0.7), thus reflecting

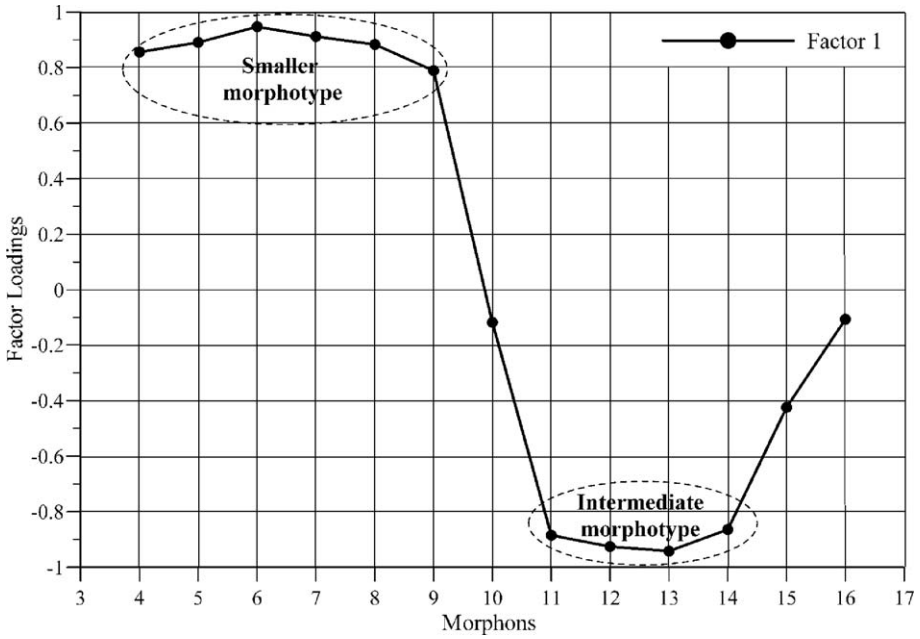

Fig. 5. F1 loadings for the several morphons for the Heinrich Layer 1 sample set (this analysis was performed on 58 samples). Extraction: Principal factors (comm.=multiple *R*-square) with varimax raw.

again the behaviour of the larger morphotype during this time interval.

4.2. *C. pelagicus (s. l.) behaviour through core MD95-2040*

4.2.1. *Overall MD95-2040 core*

Further study consisted of plotting and analysing the small/intermediate morphotype relationship (F1 factor scores) against depth, together with the two cold water proxies, the planktonic foraminifera *N. pachyderma* (sin.) and IRD, obtained from previous studies (de Abreu, 2000; de Abreu et al., 2003) (Fig. 8). Although Factor 1 represents the opposite behaviour between the smaller and the intermediate coccolith bearing morphotypes, its scores can be interpreted as an indication of the relative importance of *C. pelagicus* subsp. *pelagicus* in a region that otherwise registers the development of *C. pelagicus* subsp. *braarudii*.

Table 2
Factor loadings for Heinrich Layer 1 sample set

Variable	Factor 1
Morphon 4	0.8563*
Morphon 5	0.8908*
Morphon 6	0.9470*
Morphon 7	0.9119*
Morphon 8	0.8835*
Morphon 9	0.7888*
Morphon 10	−0.1178
Morphon 11	−0.8848*
Morphon 12	−0.9252*
Morphon 13	−0.9415*
Morphon 14	−0.8641*
Morphon 15	−0.4242
Morphon 16	−0.1063
Expl. var.	8.1351
Prp. tot.	0.6258

Extraction: Principal factors (comm.=multiple *R*-square) with varimax raw.
Marked loadings (*) are >|0.7|.

In general, factor scores show increments during cold MIS 2, 4, and 6, being the most important peaks coincidal with the highest peaks of the other proxies, associated with the Heinrich Layers (e.g. HL1 and HL6). A gradual increase of these scores is also observed from Termination II to the beginning of isotope interglacial stage 5 (Eemian), although it does not completely match the records of the other two proxies for cold water masses.

Thus, there is a positive moderate correlation between Factor 1 scores and *N. pachyderma* (sin.) ($r=0.57$; $n=84$), while with IRD this correlation, although positive, is less important ($r=0.37$; $n=84$) for the entire time series.

4.2.2. *Heinrich Layer 1*

During HL1 (Fig. 8a) the relative abundances of *N. pachyderma* (sin.) and *C. pelagicus* subsp. *pela-*

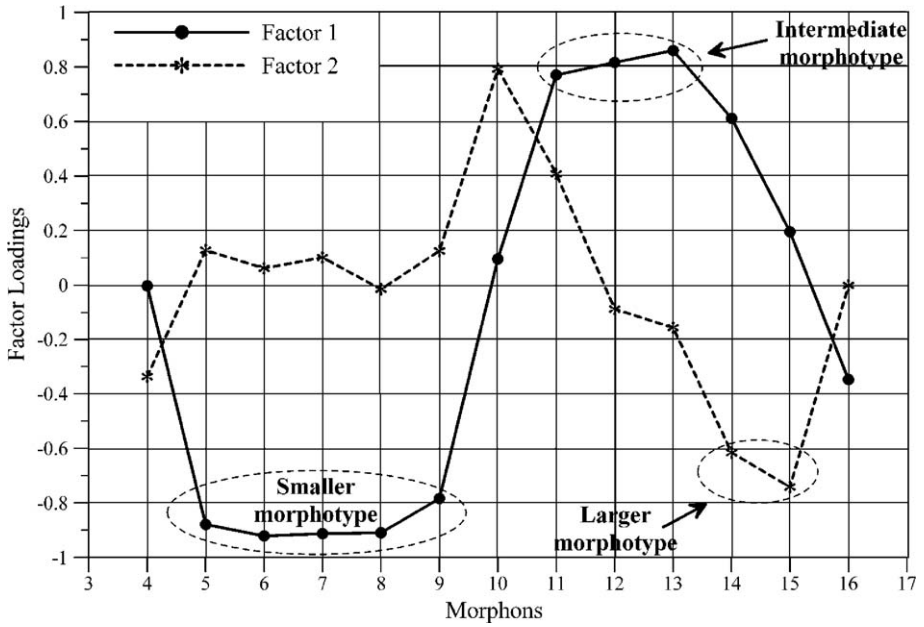

Fig. 6. F1 and F2 loadings for the several morphons for the Heinrich Layer 6 sample set (this analysis was performed on 34 samples). Extraction: Principal factors (comm. = multiple *R*-square) with varimax raw.

gicus present a very similar pattern, which is also demonstrated by the high correlation between them ($r = 0.93$; Table 5a). When compared with these two proxies, the IRD record presents, in general, a similar trend, although with more pronounced oscillations. As expected, the correlation coefficients between the two first proxies and IRD are lower, although still representative (Table 5a). The comparison of the different records allows to distinguish three phases:

- phase I is characterized by a precocious increase of *N. pachyderma* (sin.) and *C. pelagicus* subsp. *pelagicus* relative to the record of the IRD, synchronously with the onset of the cooling trend (SSTs; see Fig. 8);
- phase II, corresponding to the interval between 17.5 and 15.6 kyr for which the estimated SSTs (Fig. 8) register the lowest values, is characterized by all three proxies being persistently and abundantly represented. The oscillating pattern of IRD is responsible for the lower coefficient correlation values between this proxy and the other two (Table 5b);
- phase III is characterized by all three proxies disclosing a similar decreasing behaviour until the end of this interval, at which interpreted SSTs (Fig. 8) rise again. The representativity of their correlation is expressed by coefficient values on Table 5b.

Table 3
Factor loadings for Heinrich Layer 6 sample set

Variable	Factor 1	Factor 2
Morphon 4	−0.0029	−0.3367
Morphon 5	−0.8788*	0.1282
Morphon 6	−0.9205*	0.0622
Morphon 7	−0.9124*	0.1016
Morphon 8	−0.9092*	0.0149
Morphon 9	−0.7838	0.1254
Morphon 10	0.0959	0.7925*
Morphon 11	0.7706*	0.4085
Morphon 12	0.8166*	−0.0875
Morphon 13	0.8603*	−0.1562
Morphon 14	0.6118	−0.6154
Morphon 15	0.1956	−0.7416*
Morphon 16	−0.3479	−0.0012
Expl. var.	6.4366	1.9155
Prp. tot.	0.4951	0.1473

Extraction: Principal factors (comm. = multiple *R*-square) with varimax raw.
Marked loadings (*) are >|0.7|.

4.2.3. Heinrich Layer 6

During HL6 (Fig. 8b) the *N. pachyderma* (sin.) and *C. pelagicus* subsp. *pelagicus* relative predominance also depicts a similar but less close pattern in three

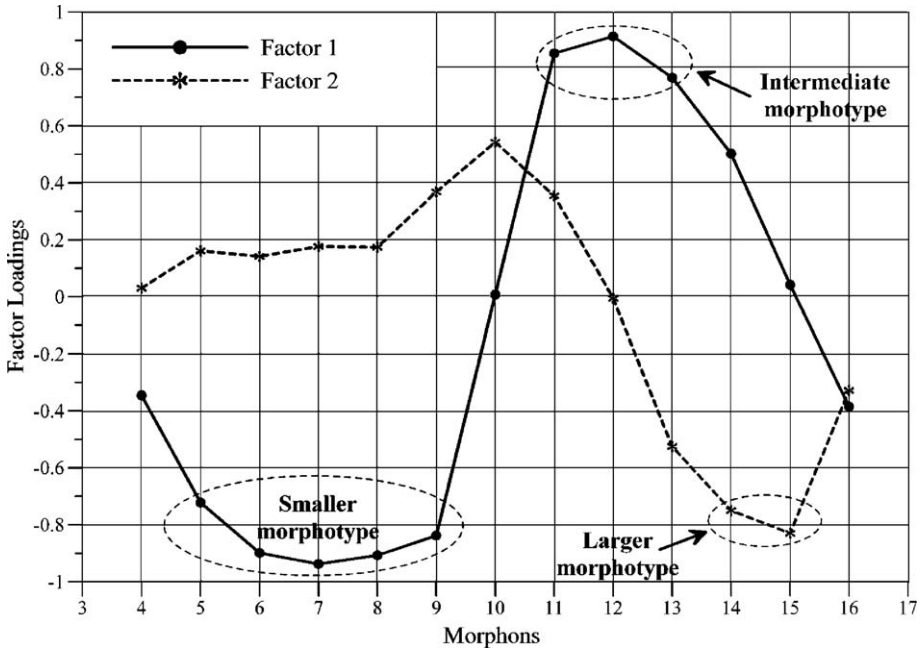

Fig. 7. F1 and F2 loadings for the several morphons for the interval TII-Eemian sample set (this analysis was performed on 51 samples). Extraction: Principal factors (comm. = multiple *R*-square) with varimax raw.

phases. In fact, the correlation among the three proxies is representative for the overall interval, but with negative values between *C. pelagicus* subsp. *pelagicus* and the other two proxies (Table 6a).

– phase I, as during HL1, *N. pachyderma* (sin.) and *C. pelagicus* subsp. *pelagicus* reacted to the cooling shortly before the arrival of IRD. Due to the reduced number of samples, correlations although high are not meaningful (Table 6a);
– phase II, displaying the lowest estimated SSTs (Fig. 8, time interval 61.4 to 59 kyr), and in spite of the three proxies being well represented and with an overall similar trend, correlations are low and not meaningful (Table 6b). Thus, *C. pelagicus* subsp. *pelagicus* relative abundance exhibits a pattern with relatively strong oscillations, namely at the base and the top of these interval peaks, which moderately correspond to the major peaks of the IRD record. Similarly, a non-meaningful anti-variation between *C. pelagicus* subsp. *pelagicus* and *N. pachyderma* (sin.) might indicate a moderate offset between these two proxies;
– phase III is characterized by a synchronous decrease on the abundance of the three proxies. Although showing an identical behaviour only the positive correlation between *N. pachyderma* (sin.) and IRD record is meaningful (Table 6b).

Table 4
Factor loadings for the interval TII-Eemian sample set

Variable	Factor 1	Factor 2
Morphon 4	−0.3457	−0.0301
Morphon 5	−0.7218*	0.1610
Morphon 6	−0.8989*	0.1417
Morphon 7	−0.9376*	0.1767
Morphon 8	−0.9070*	0.1735
Morphon 9	−0.8381*	0.3683
Morphon 10	0.0075	0.5426
Morphon 11	0.8550*	0.3545
Morphon 12	0.9146*	−0.0055
Morphon 13	0.7693*	−0.5254
Morphon 14	0.5027	−0.7500*
Morphon 15	0.0418	−0.8298*
Morphon 16	−0.3850	−0.3283
Expl. var.	6.4149	2.2987
Prp. tot.	0.4935	0.1768

Extraction: Principal factors (comm. = multiple *R*-square) with varimax raw.
Marked loadings (*) are >|0.7|.

4.2.4. Termination II-Eemian

From Termination II to the beginning of isotope interglacial stage 5 (Eemian), the relative behaviour of *C. pelagicus* subsp. *pelagicus* does not accompany the records of the other two proxies (Fig. 8c). This decoupling is responsible for the registered null correlations

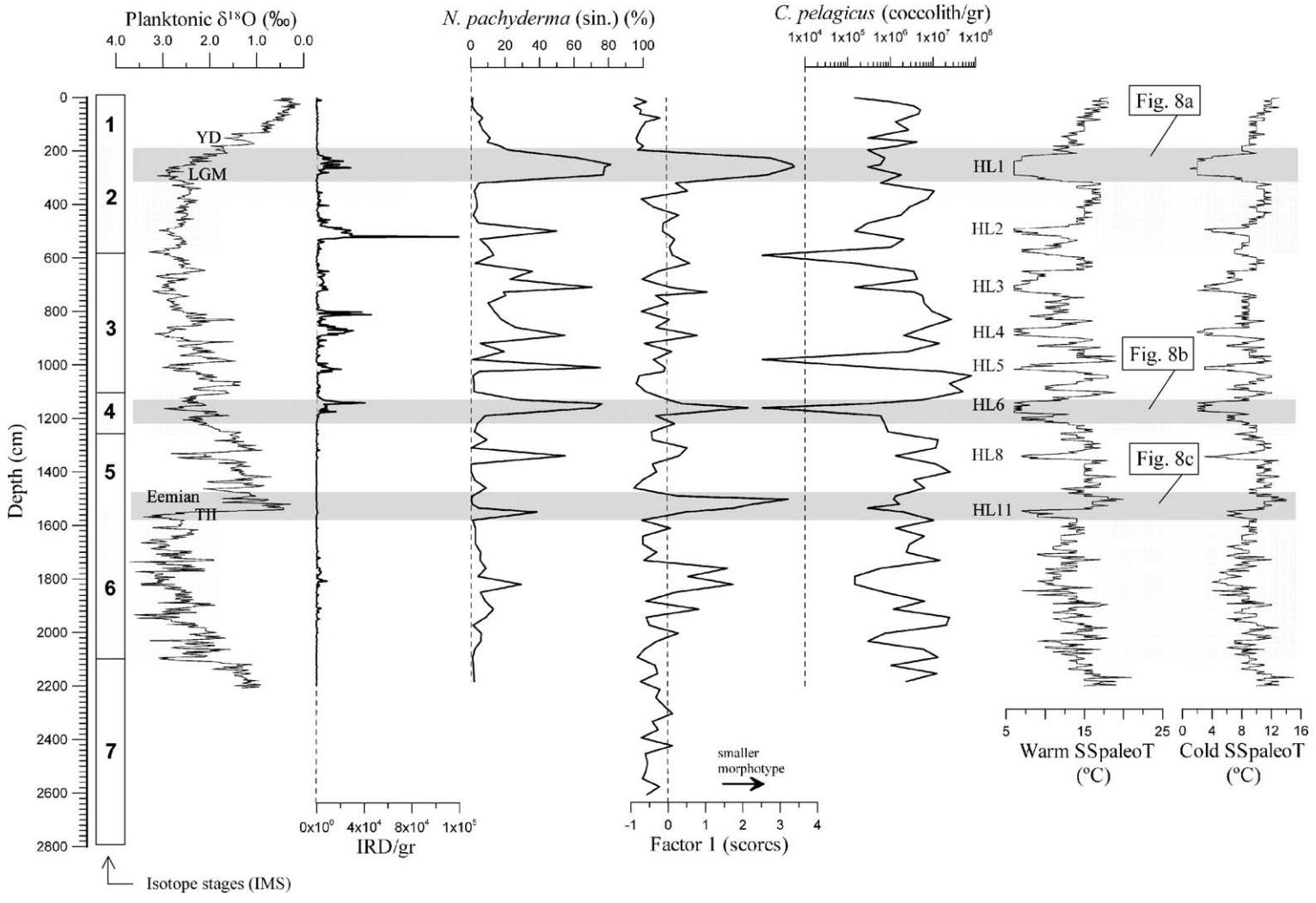

Fig. 8. Comparison of the relative importance of *C. pelagicus* subsp. *pelagicus* (Factor 1) with the records of the planktonic foraminifera *N. pachyderma* (sin.), IRD (de Abreu, 2000; de Abreu et al., 2003) and of the absolute abundance (coccolith/gr) of *C. pelagicus* (s. l.) (Parente et al., 2004). Planktonic $\delta^{18}O$ (*G. bulloides*) and estimated SSTs (de Abreu, 2000) are also shown. Grey bands indicate the intervals relative to the subsequent detailed studies. a—Variation of the relative importance of *C. pelagicus* subsp. *pelagicus* (Factor 1) versus age and its comparison to *N. pachyderma* (sin.) and IRD curves during the Heinrich Layer 1. (Age model from de Abreu et al., 2003); b—Variation of the relative importance of *C. pelagicus* subsp. *pelagicus* (Factor 1) versus age and its comparison to *N. pachyderma* (sin.) and IRD curves during the Heinrich Layer 6 (age model from de Abreu et al., 2003); c—Variation of the relative importance of *C. pelagicus* subsp. *pelagicus* (Factor 1) versus age and its comparison to *N. pachyderma* (sin.) and IRD curves during the interval TII-Eemian (age model from de Abreu et al., 2003).

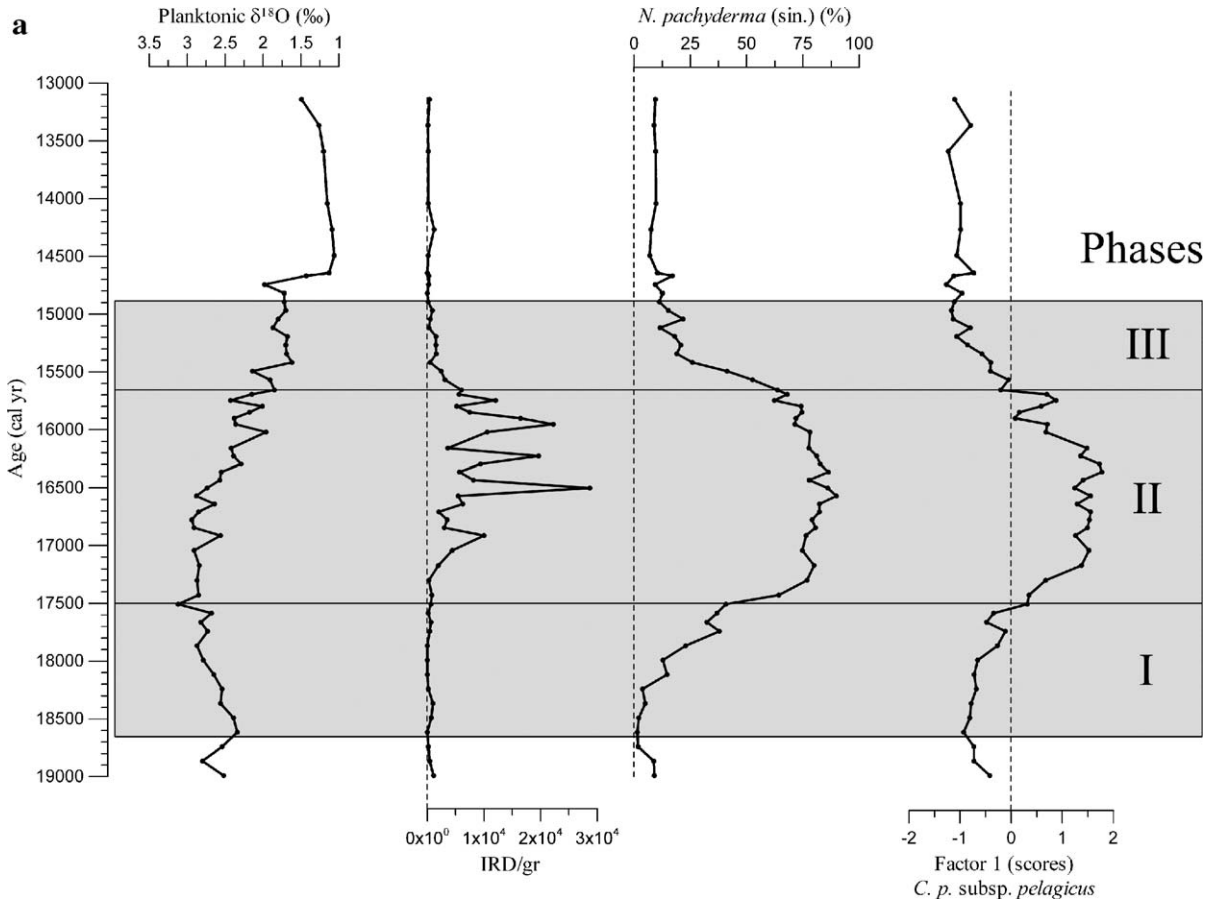

Fig. 8 (*continued*).

(Tables 7a, b and c). In this interval five different phases can be observed:

- phase I, as during the previous intervals, is characterized by the simultaneous increase of *N. pachyderma* (sin.) and *C. pelagicus* subsp. *pelagicus*, both registering the cooling trend earlier than IRD;
- phase II, from 134 to 125 kyr, both IRD and *N. pachyderma* (sin.) display a significant increase timidly followed by *C. pelagicus* subsp. *pelagicus*;
- phase III is defined this time by lower and irregular IRD values and almost null *N. pachyderma* (sin.) percentages, while *C. pelagicus* subsp. *pelagicus* continuous to increase its record;
- phase IV, from 117.6 to 114.8 kyr, *N. pachyderma* (sin.) and IRD are almost absent while *C. pelagicus* subsp. *pelagicus* is still increasing its importance;
- phase V defines the interval during which *C. pelagicus* subsp. *pelagicus* relative abundance returns to minimal values.

This complete decoupling between *C. pelagicus* subsp. *pelagicus* and the other proxies are well depicted by their correlation values for phases II to V, though during phase I, as mentioned, *C. pelagicus* subsp. *pelagicus* and *N. pachyderma* (sin.) behaved similarly.

5. Discussion

5.1. Importance of the Multivariate Morphon Analysis (MMA)

By tabulating morphometric measurements of *C. pelagicus* (s. l.) placoliths into 1.0 μm classes (morphons 4 to 16 μm), MMA disclosed clusters of mutually correlated contiguous morphons, each cluster defining a single morphotype.

Concerning the definition of morphotype boundaries, our data indicates that the morphometric interval characteristic of each morphotype narrows from the smaller to the larger morphotype (Fig. 9), although small changes in time may occur. For instance, during HL1

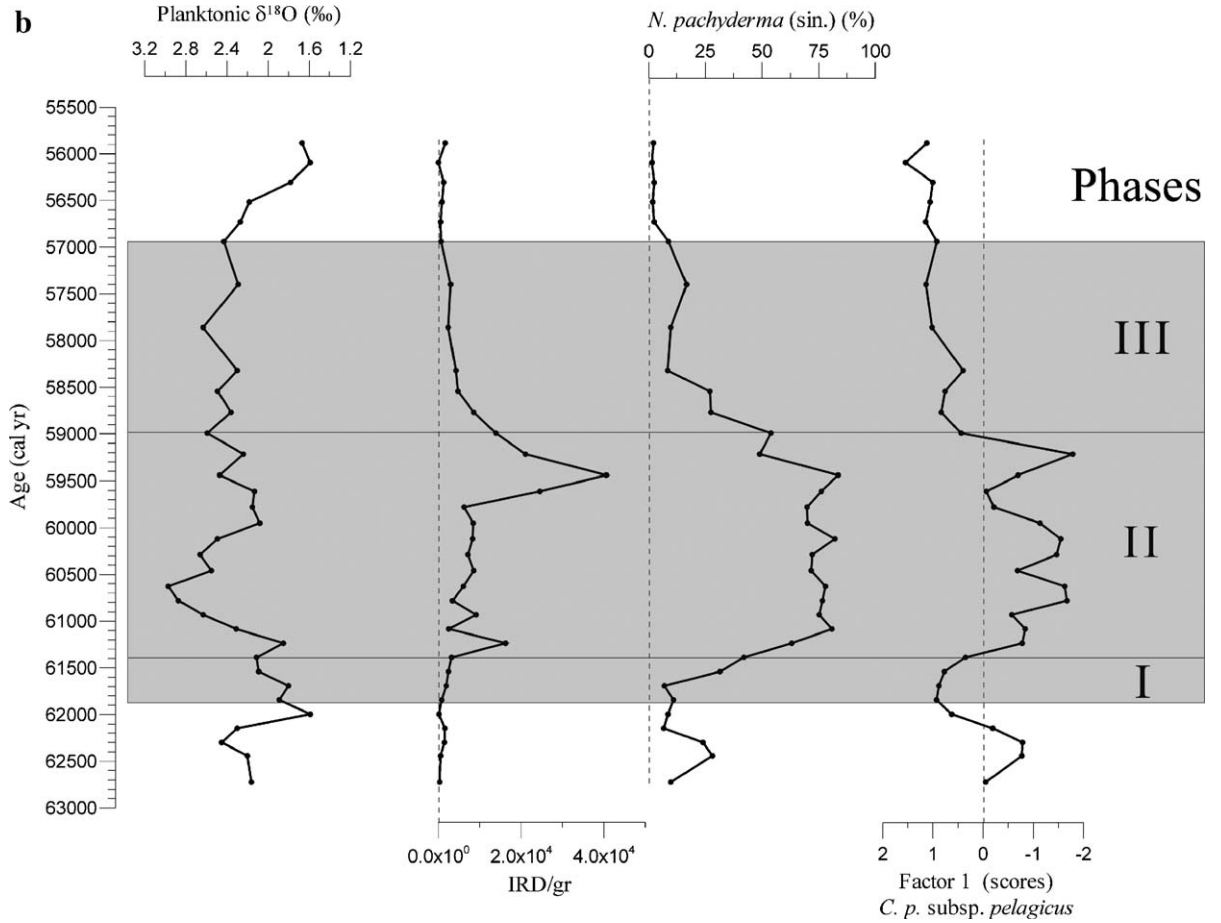

Fig. 8 (*continued*).

(Fig. 5), the smaller morphotype is defined by a strong correlation between all morphons 4 to 9, indicating that all placoliths between 4 and 10.0 μm equally contribute to its definition. However, during HL6 (Fig. 6), morphon 4 (placoliths with [4.0; 5.0[μm length) do not correlate with the others and so should not be used to define it. Causes for this can be related to its lower abundance because: i) it was not well formed during this older cold stage or ii) its presence in the region was too erratic. During TII-E (Fig. 7) morphon 4 regained some importance for the definition of the smaller morphotype. However, its factorial load being less than $|-0.4|$) means that a significant part of the measured specimens with that size range have no correlation with the rest of the cluster, and thus should not be used for the morphotype tabulation. As shown, which of these specimens covary and thus can be used with the rest to define a specific morphotype can only be defined through MMA.

Results show that during these three time slices the upper morphometric limit between the smaller and the intermediate morphotypes is kept consistently around the size range of morphon 10 ([10.0; 11.0[μm), as displayed by its almost null factor loadings (see Figs. 5–7). Thus, this dimensional interval reveals to be useful to separate placoliths attributed to *C. pelagicus* subsp. *pelagicus* and *C. pelagicus* subsp. *braarudii*, respectively, confirming previous interpretations from Geisen et al. (2002).

During HL1 a single factor explains the overall morphometric behaviour of *C. pelagicus* (s. l.), indicating that only the smaller and intermediate morphotypes are present, with a clear opposite behaviour between them (see Fig. 5). This allows a simpler comparison of the MMA method with the more traditional single histogram visual analysis. As seen in Fig. 10, frequency histograms clearly display the 10 μm morphometric boundary. Samples 293 and 218 cm have low F1 scores meaning that the two morphotypes have an equal importance as shown by their histograms. Sample 257 cm has a higher positive score. Since the higher positive loadings of Factor 1 characterize the smaller morphotype, high positive

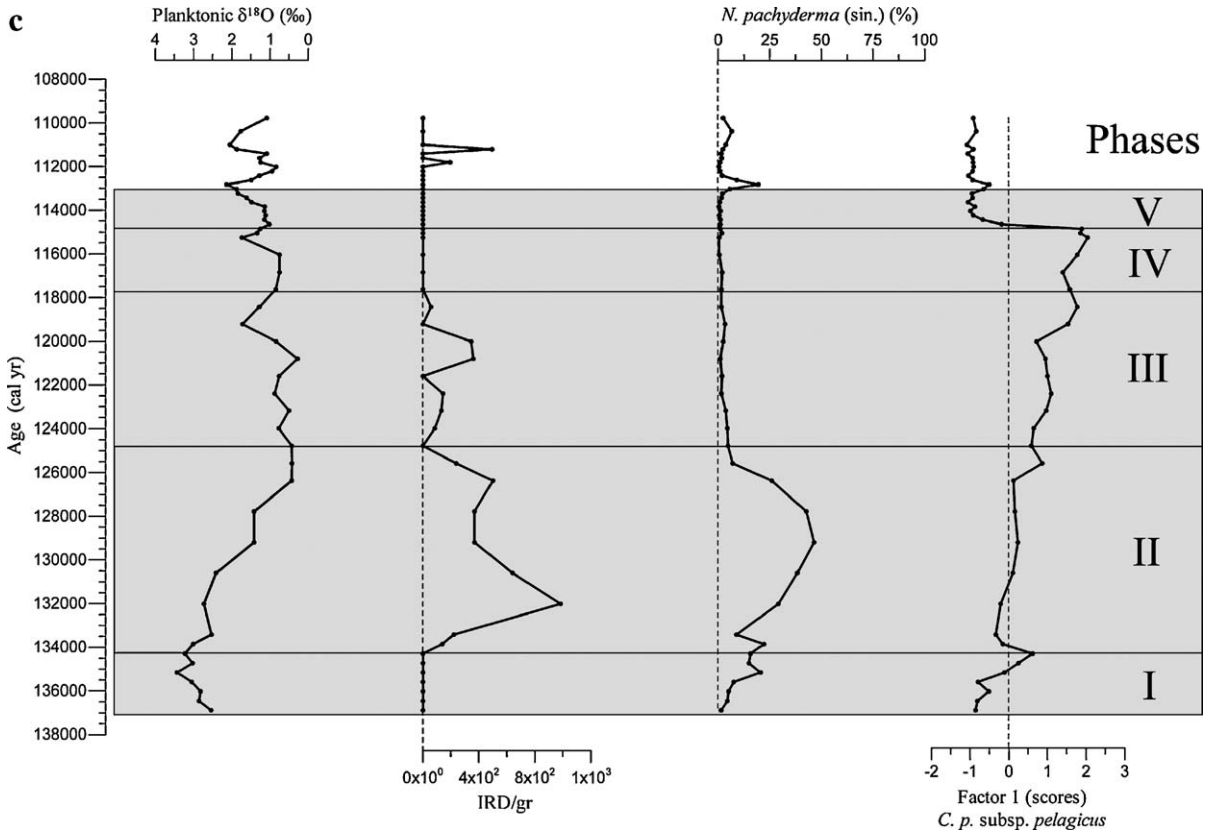

Fig. 8 (*continued*).

scores indicate this form is better represented than the intermediate morphotype. Sample 185 cm, on the other hand, has a relatively high negative score. Since the negative loadings of F1 are related to the intermediate *C. pelagicus* subsp. *braarudii* morphotype, this form should be better represented relative to the entire range sizes, as clearly seen by its histogram.

Table 5a
Correlation coefficient values (r) among ice-rafted detritus (IRD), *N. pachyderma* (sin.) and *C. pelagicus* subsp. *pelagicus* during the entire Heinrich Layer 1 and the first phase of this interval

	IRD	*N. pachyd.*	*C. p. p.*	
IRD		**$r = 0.63$** $n = 58$	**$r = 0.55$** $n = 58$	HL1 Overall
N. pachyd.	$r = 0.2$ $n = 10$		**$r = 0.93$** $n = 58$	
C. p. p.	$r = 0.21$ $n = 10$	**$r = 0.91$** $n = 10$		
	HL1 Phase I			

Bold correlations are significant at $p < 0.05$.

Table 5b
Correlation coefficient values (r) among ice-rafted detritus (IRD), *N. pachyderma* (sin.) and *C. pelagicus* subsp. *pelagicus* during the second and third phases of the Heinrich Layer 1

	IRD	*N. pachyd.*	*C. p. p.*	
IRD		$r = -0.02$ $n = 23$	$r = -0.17$ $n = 23$	HL1 Phase II
N. pachyd.	**$r = 0.85$** $n = 11$		**$r = 0.71$** $n = 23$	
C. p. p.	**$r = 0.68$** $n = 11$	**$r = 0.82$** $n = 11$		
	HL1 Phase III			

Bold correlations are significant at $p < 0.05$.

Table 6a
Correlation coefficient values (r) among ice-rafted detritus (IRD), *N. pachyderma* (sin.) and *C. pelagicus* subsp. *pelagicus* during the entire Heinrich Layer 6 and the first phase of this interval

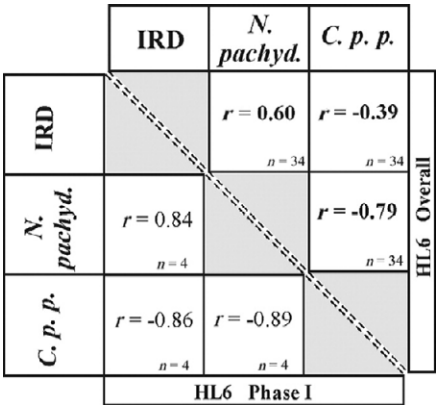

Bold correlations are significant at $p < .05$.

Table 7a
Correlation coefficient values (r) among ice-rafted detritus (IRD), *N. pachyderma* (sin.) and *C. pelagicus* subsp. *pelagicus* during the entire interval TII-Eemian and its first phase

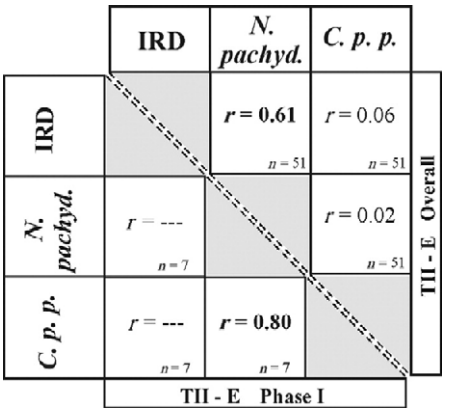

Bold correlations are significant at $p < 0.05$.

Intermediate stages in the steps described above were not presented for the sake of clarity. In fact, the analysis and graphic representation of a large number of histograms altogether is cumbersome and is one of the advantages of substitution by the integrated approach provided by the MMA method. However, because the MMA method is based on "the behaviour of the sizes" it can not be applied to isolated or to a limited number of samples. The minimum number of samples should necessary be equal to the number of morphons (i.e. tabulated morphometric classes) that are considered for a specific taxa.

The usefulness of MMA is even better evidenced when one attempts to define the morphometric boundary between the intermediate and the larger morphotypes. While during HL1 *C. pelagicus* subsp. *braarudii* was formed by all morphons 11 to 14 ([11.0; 15.0[μm) (Parente et al., 2004), during HL6 (Fig. 6) the morphon 14 ([14.0; 15.0[μm) has both positive scores on Factor 1 and negative scores on Factor 2. This indicates that part of the placoliths that integrate this morphon behave coherently with the 11–14 μm sized placoliths, which constitute *C. pelagicus* subsp. *braarudii*, while another part shows a distinct and independent behaviour in phase with the other larger placoliths, which are attributed to the larger morphotype *C. pelagicus* subsp. *azorinus*. The same also occurs during TII-E, although to a lesser

Table 6b
Correlation coefficient values (r) among ice-rafted detritus (IRD), *N. pachyderma* (sin.) and *C. pelagicus* subsp. *pelagicus* during the second and third phases of the Heinrich Layer 6

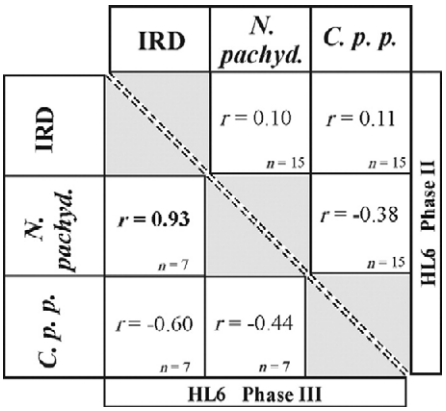

Bold correlations are significant at $p < .05$.

Table 7b
Correlation coefficient values (r) among ice-rafted detritus (IRD), *N. pachyderma* (sin.) and *C. pelagicus* subsp. *pelagicus* during the second and third phases of the interval TII-Eemian

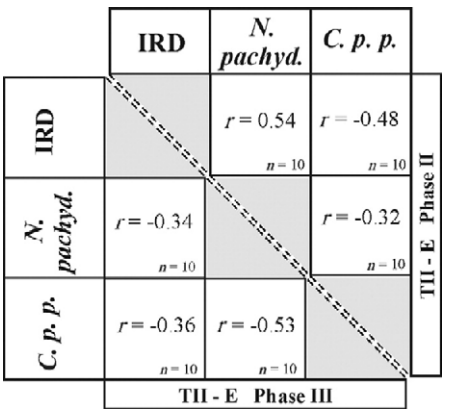

Bold correlations are significant at $p < 0.05$.

Table 7c
Correlation coefficient values (r) among ice-rafted detritus (IRD), *N. pachyderma* (sin.) and *C. pelagicus* subsp. *pelagicus* during the fourth and fifth phases of the interval TII-Eemian

	IRD	*N. pachyd.*	*C. p. p.*	
IRD		r = --- n = 7	r = --- n = 7	TII - E Phase IV
N. pachyd.	r = -0.08 n = 21		r = -0.07 n = 7	
C. p. p.	r = -0.07 n = 21	r = 0.35 n = 21		
	TII - E Phase V			

Bold correlations are significant at $p < 0.05$.

degree. This indicates that the morphometric boundary between the intermediate and the larger morphotypes is less clearly defined due to a higher degree of overlapping between them (Fig. 9), which, in turn, may reflect a younger phylogenetic separation. In these circumstances, to distinguish these morphotypes based only on single histograms is virtually impossible. Fig. 11 shows the relative behaviour of the three morphotypes during HL6, expressed by their respective MMA factorial scores and selected frequency histograms. Sample 1187 cm has a positive F1 score and a negative F2 score. As shown before (see Fig. 6) this indicates a strong presence of both the intermediate and the larger morphotypes. In fact, the histogram shows a minor contribution of the smaller morphotype relative to the larger placoliths (11 to 15 μm), but do not show a clear distinction between the larger morphotypes. As stated before, this latter distinction can only be made by analysing the behaviour of the morphons along the selected time series, and not on a single sample. The following selected sample (1160 cm) has a negative F1 score and a positive F2 score. As shown before this indicates that the smaller morphotype is better represented than the intermediate morphotype (as clearly shown by its histogram), and the larger morphotype should be absent. This last aspect is less clear to observe in the histogram of the sample 1160 cm, mainly because Factor 2 is also influenced by the presence of placoliths of size [10,11[, which MMA analysis indicates do not contribute to the smaller neither to the intermediate morphotypes, but anti-vary with the largest sized placoliths, a still not completely understood relationship. The almost null F1 scores for sample 1148 cm is indicative of the equatitative presence of the smaller and the intermediate morphotypes, an aspect that is clearly seen in the histogram. As for sample 1187 cm its negative F2 scores also indicate the presence of the large morphotype. Positive F1 and F2 scores for sample 1136 cm are indicative of increased importance of the intermediate morphotype, relative to the others. The last selected sample (1106 cm) is a more extreme situation than those previously described as its histogram also clearly shows.

5.2. Palaeoecological and palaeoceanographical implications

5.2.1. Comparison *C. pelagicus subsp. pelagicus* versus *C. pelagicus subsp. braarudii*

Several mechanisms have been proposed to explain the iceberg discharges into the North Atlantic, known as “Heinrich events” (Broecker et al., 1992), such as insulation changes (Heinrich, 1988), sea level changes (Bond and Lotti, 1994), global temperature changes (Bond and Lotti, 1995), and ice-sheet dynamics (Broecker, 1994; McManus et al., 1999). During the subsequent trend to increase global tem-

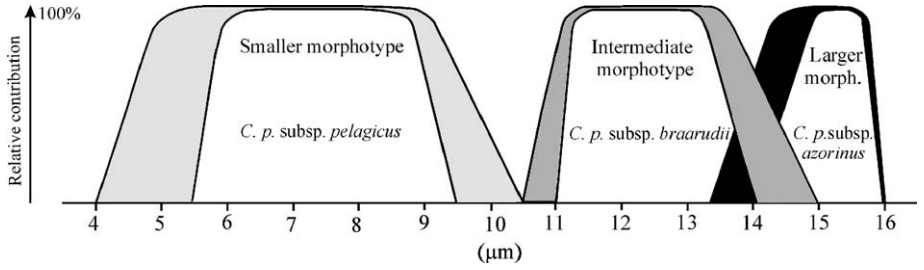

Fig. 9. Diagram illustrating the relative contribution and variability of *C. pelagicus* (s. l.) placolith lengths for the three morphotypes. The dimensional interval that characterizes them decrease from the smaller to the larger morphotype, while the dimensional boundary between the smaller and the intermediate morphotypes is much better defined than between the intermediate and the larger ones.

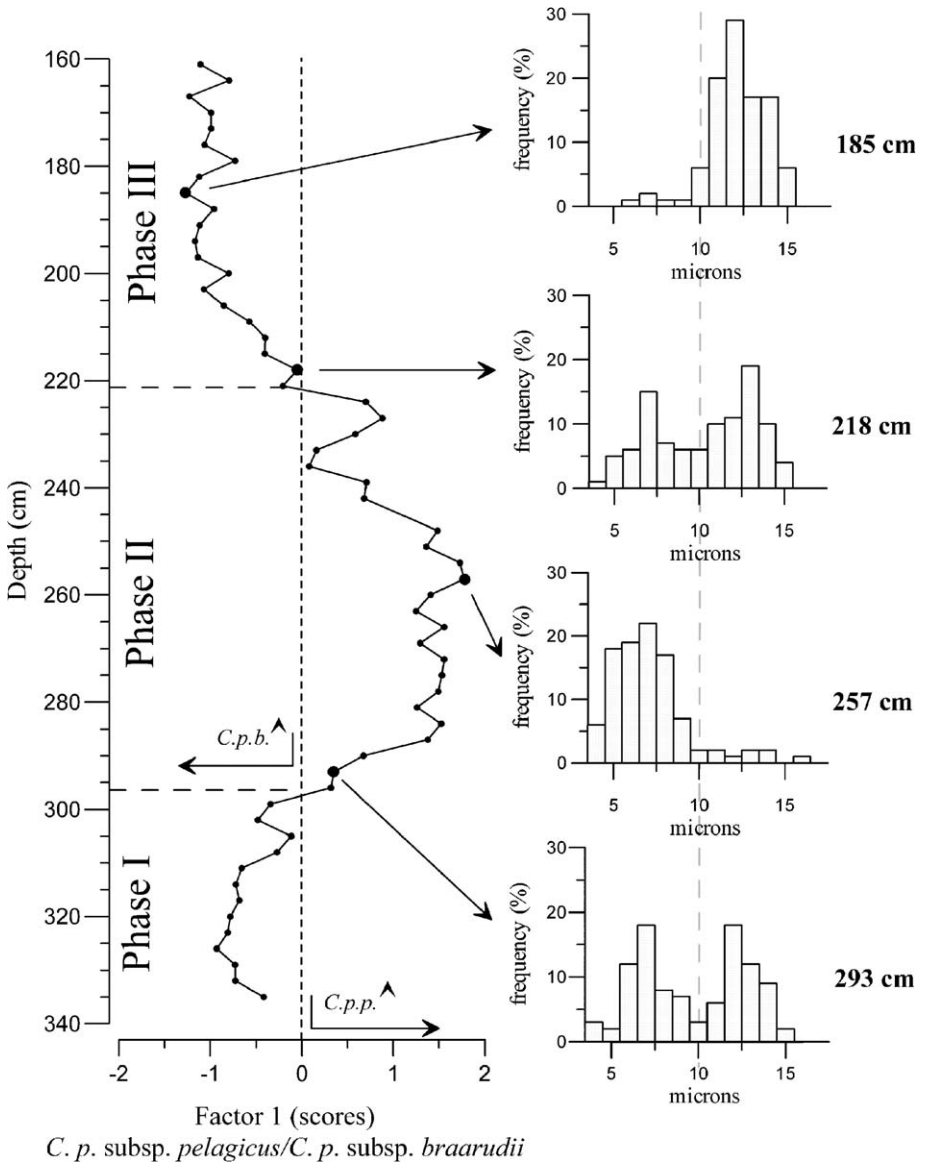

Fig. 10. Time series and histograms of Factor 1 scores for HL1 for selected samples (293, 257, 218 and 185 cm). Positive scores indicate a stronger presence of *C. pelagicus* subsp. *pelagicus* (*C.p.p.* ↑ —*C. pelagicus* subsp. *pelagicus* increase). Negative scores indicate a stronger presence of *C. pelagicus* subsp. *braarud*ii (*C.p.b.* ↑ —*C. pelagicus* subsp. *braarudii* increase). Samples with almost null scores are characterized by the presence of both subspecies.

perature, the southward migration and melting of icebergs at medium latitudes as indicated by several evidences (Cayre et al., 1999; Bard et al., 2000; de Abreu et al., 2003) would induce the cooling of the surrounding water masses. Entire coccospheres (or just isolated placoliths) of *C. pelagicus* subsp. *pelagicus* may thus have extended its geographic range, towards the Iberian margin reflecting this cold water influx.

The systematic increment of *C. pelagicus* subsp. *pelagicus* over *C. pelagicus* subsp. *braarudii* during Heinrich events shows that their opposite behaviour, expressed throughout the last 200 kyr of core MD95-2040 by MMA F1 scores (see Figs. 3, 5, 6 and 7), can be used as a proxy for cold waters, similarly to the record of *N. pachyderma* (sin.) and IRD. This is corroborated by negative correlations, although moderate, between F1 scores and estimated palaeotemperatures ($r=-0.51$ and $r=-0.43$ for cold and warm season SSTs, respectively).

The consistently opposite behaviour between *C. pelagicus* subsp. *pelagicus* and *C. pelagicus* subsp.

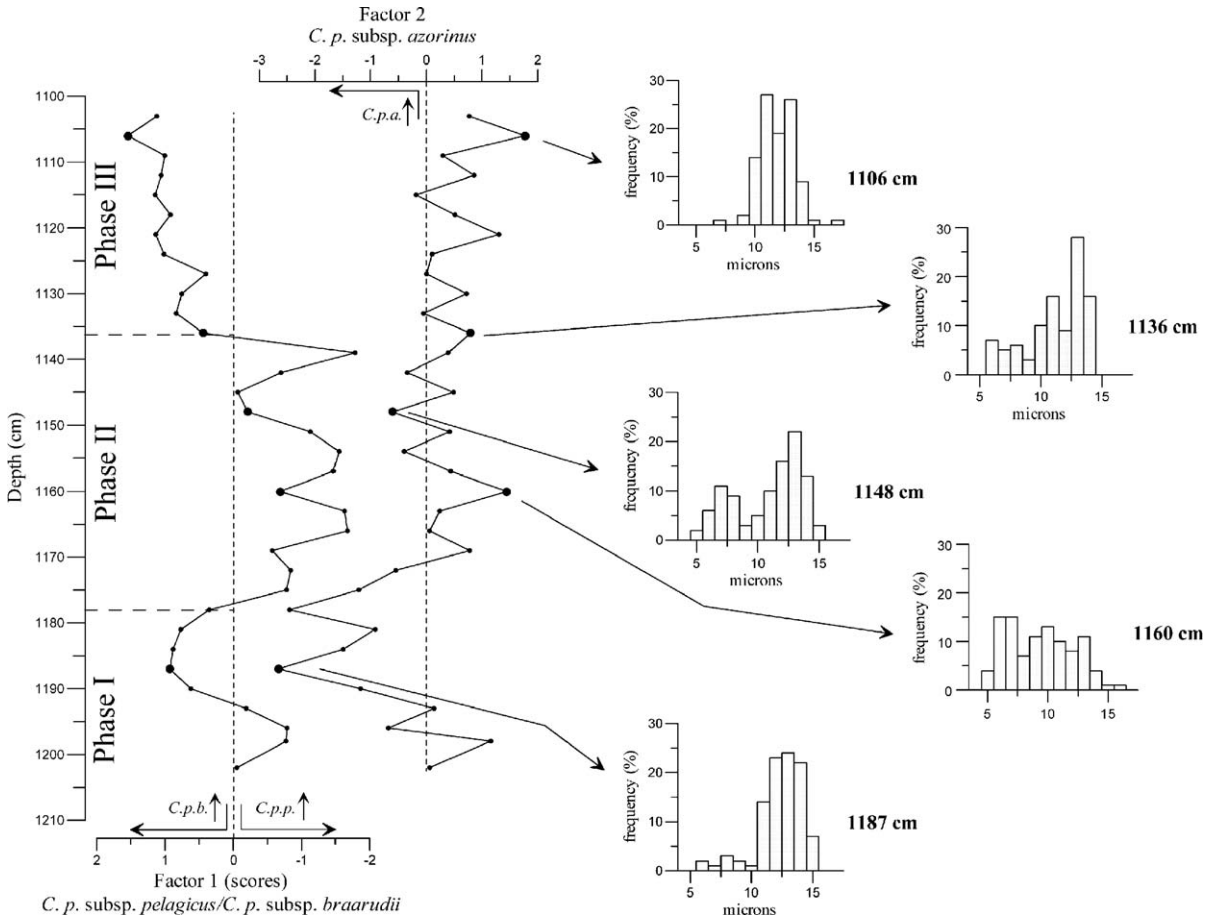

Fig. 11. Time series and histograms of Factor 1 and Factor 2 scores for HL6 for selected samples (1187, 1160, 1148, 1136 and 1106 cm). Positive F1 scores indicate a stronger presence of *C. pelagicus* subsp. *braarudii* (*C.p.b.*↑—*C. pelagicus* subsp. *braarudii* increase). Negative F1 scores indicate a stronger presence of *C. pelagicus* subsp. *pelagicus* (*C.p.p.*↑—*C. pelagicus* subsp. *pelagicus* increase). Samples with almost null F1 scores are characterized by the presence of these both subspecies. Negative F2 scores indicate a stronger presence of *C. pelagicus* subsp. *azorinus* (*C.p.a.*↑—*C. pelagicus* subsp. *azorinus* increase).

braarudii off the Western Iberia margin is interpreted as follows. During glaciations the southward shift of the Polar Front closer to North Iberia moved the meridional limit of the ecological niche of *C. pelagicus* subsp. *pelagicus* southwards. This shift seemed to have conditioned at certain specific moments the development of *C. pelagicus* subsp. *braarudii*, which otherwise was experiencing a fair development due to on one hand an increase on upwelling conditions during glacial times and on the other hand a restriction by sea level retreat from the Western Iberia continental shelf, over which has its present day niche. Thus, while the presence of the smaller morphotype off Western Iberia is linked to a cooling trend, the intermediate morphotype (*C. pelagicus* subsp. *braarudii*) seems to be favoured by non-glacial upwelling conditions (see Cachão and Moita, 2000). The behaviour of the larger morphotype (when present) is always characterized by a distinct factor, reflecting that its behaviour is unrelated to the others and thus its presence off Iberia must be linked to a distinct mechanism, most probably related to the activity of the Azores Front (Parente et al., 2004).

5.2.2. Comparison *C. pelagicus subsp. pelagicus* versus *N. pachyderma (sin.)* and IRD

Since *N. pachyderma* (sin.) and IRD (Fig. 8) are commonly used to better characterize periods influenced by cold meltwater, the significant overall similarity of F1 scores to the records of these two proxies, particularly evident during MIS 2 and 4, confirms the positive response of *C. pelagicus* subsp. *pelagicus* to the arrival of subpolar water masses off Western Iberia. The limited contribution of *C. pelagicus* subsp. *pela-*

gicus to MIS 6 when compared to MIS 2 and 4, as also registered by *N. pachyderma* (sin.) percentages (de Abreu et al., 2003), corroborates earlier interpretations suggesting a reduced southward influence of polar water masses at that time (e. g. Lebreiro et al., 1996, 1997; Cayre et al., 1999; Calvo et al., 2001).

Detailed analysis for the HL1, HL6 and TII-Eemian intervals occasionally show small discrepancies in the timings of these three proxies. This can be partially understood if one considers that the present day occurrence of sinistral *N. pachyderma* is mainly confined to the Polar region itself (e.g. Hemleben et al., 1989; Bauch et al., 2003) while *C. pelagicus* subsp. *pelagicus* is attributed to the bordering Subarctic biogeographic province (McIntyre and Bé, 1967; Raham fide Roth, 1994; Winter et al., 1994). Since the two taxa do not share the exact same water masses their records may reflect the position of their respective biogeographical boundaries.

For all three studied time intervals (HL1, HL6 and TII-E) the increase of both *C. pelagicus* subsp. *pelagicus* and *N. pachyderma* (sin.) shortly before the rise of IRD abundances (bottom of phase I; see Fig. 8a,b and c) is interpreted as reflecting an increase in the cooling trend and maximum meridional ice front development, which gradually shifted southwards their subpolar and polar meridional biogeographic boundaries. Their synchronicity indicates, on the other hand, that during this paroxysmal cold stage (phase I) the meridional limits of the Planktonic Foraminiferal Polar and the Calcareous Nannoplankton Subarctic Zones coincided, while migrating over our core location, off Western Iberia. This overlapping is also confirmed by high correlations between F1 scores and *N. pachyderma* (sin.) during all phase I (see Tables 5a, 6a and 7a). With the onset of terminations, ice cap break up and southward movement of the iceberg armadas, IRD begins to arrive at our core location, and defines the lower limit of all phase II. During this stage, both *C. pelagicus* subsp. *pelagicus* and *N. pachyderma* (sin.) increase significantly their relative abundance, reflecting an enlargement of their biogeographic domains in this region. During HL1 *C. pelagicus* subsp. *pelagicus* and *N. pachyderma* (sin.) records of phase II correlate with each other significantly ($r = 0.71$; Table 5b) but between *C. pelagicus* subsp. *pelagicus* and IRD it is not so good. This seems to indicate that, at this stage, both types of organisms shared the same palaeobiogeography but were not favoured during direct iceberg discharges. However, during all phase II of HL6 and TII-E, *C. pelagicus* subsp. *pelagicus* and *N. pachyderma* (sin.) display negative moderate correlation to each other. Although sharing the same palaeobiogeography, it is interpreted that they developed in distinct water masses, keeping their own identity, as reflected by this present day distinct Northern Atlantic biogeographic provinces.

Phase III of HL1 and HL6, characterized by the gradual decreasing trend of *C. pelagicus* subsp. *pelagicus*, *N. pachyderma* (sin.) and IRD, are interpreted as reflecting the disappearance of glacial–subglacial water conditions from offshore Iberia and the re-establishment of a North Atlantic current system similar to today. Again, during HL1 all three proxies behave quite similarly (correlation coefficients are significantly high; Table 5b), while during HL6 *C. pelagicus* subsp. *pelagicus* and *N. pachyderma* (sin.) display moderate anti-variation. This suggests that during HL1 the glaciation–deglaciation cycle was much more intense than during HL6, for which either species, although reflecting the same general retreat pattern maintained their individuality of inhabiting slightly distinct water masses. Phase III of TII-E is quite distinct from the previous ones. In it IRD experiences a less intense and more irregular second increase, *N. pachyderma* (sin.) practically disappears while *C. pelagicus* subsp. *pelagicus* increases its relative abundance. This complete decoupling between the two taxa indicates that during Termination II the Planktonic Foraminiferal Polar province retreated from off Iberia much faster than the Calcareous Nannoplankton Subarctic province, sooner even than the complete iceberg meltdown. On the other hand, the Subarctic province persisted much longer than for the other time intervals, as indicated by the increasing pattern of *C. pelagicus* subsp. *pelagicus* even when the other two proxies were already absent (phase IV). This is interpreted as reflecting a much slower return to normal conditions after TII around Western Iberia, compared to what happened during Termination I (HL1). This interpretation implies that obtained SST's for this interval along Western Iberia are overestimated due to the precocious retreat of *N. pachyderma* (sin.), one of their transfer function estimators.

Finally 7.6 kyr after the *N. pachyderma* (sin.) and 2.8 kyr after the IRD, *C. pelagicus* subsp. *pelagicus* disappears from this latitude (phase V).

The above interpretations fail, however, to justify the reason why other Heinrich Layers (HL 2 and 5) present a significant increase of *N. pachyderma* (sin.) and IRD but no meaningful record of *C. pelagicus* subsp. *pelagicus*. This question will continue to be followed through the undergoing study of new cores in the region.

6. Conclusion

From the results of the statistical morphometric analysis of *C. pelagicus* (s. l.), here defined as Multivariate Morphon Analysis (MMA), applied to core MD95-2040 located off Western Iberia, a small morphotype (with coccolith lengths less than 10.0 μm) known as *C. pelagicus* subsp. *pelagicus* could be recognized. This taxon depicted in all situations a clear anti-variation to *C. pelagicus* subsp. *braarudii* as expressed by the most important factor retrieved by MMA. F1 scores revealed an overall similar response to *N. pachyderma* (sin.) and IRD and thus have a potential to be used as a palaeoceanographic proxy for the influence of Subpolar North Atlantic water masses. However, when analysed in much greater detail, the coupling or decoupling between *C. pelagicus* subsp. *pelagicus* and the other two cold water proxies allows more precise palaeoceanographic local reconstructions. Thus, for each of the three higher resolution sections (Heinrich Layer 1, Heinrich Layer 6 and the interval from Termination II to the Eemian) we conclude that:

1. The significantly coupling (in phase and positively correlated) between *C. pelagicus* subsp. *pelagicus* and *N. pachyderma* (sin.) during HL1, together with the fact that the morphometric variability of *C. pelagicus* subsp. *pelagicus* is mainly explained by a single factor, indicates that the Last Glacial Maximum and Termination I strongly conditioned palaeoecological conditions off Western Iberia, during which there seems to be an overlapping of both Polar and Subarctic biogeographic provinces;
2. The moderate decoupling (in phase but slightly negatively correlated) of *C. pelagicus* subsp. *pelagicus* and *N. pachyderma* (sin.) during HL6, together with a more complex pattern of morphometric variability, indicates that during HL6 the cooling phase was intense but the warming occurred more gradually, allowing the two taxa to retreat to the global changing conditions but according to their own specific slightly distinct (palaeo)ecological requirements;
3. The complete decoupling of *C. pelagicus* subsp. *pelagicus* and *N. pachyderma* (sin.) during and after TII-E indicates a much gradual return to normal interglacial conditions, in which each taxon kept their own identity. This allows a distinction to be made between the first retreat of the Polar province followed, 7.6 kyr later, by the Subarctic biogeographic domain retreat from off Western Iberia.

Acknowledgements

This work was funded by the projects CANAL (FCT POCTI/32724/99), CRIDA (FCT PLE/8/00) and SFRH/BD/8944/2002. We would like to express our acknowledgement to Professor Sir Nicholas J. Shackleton for granting access to IMAGES core MD95-2040 and to Mike Hall from the Godwin Laboratory (Cambridge) for the vast number of stable isotope measurements presented in this paper. Contribution of Bruno Ribeiro (CANAL's BTI scholarship) is also gratefully acknowledged by the authors.

References

Andruleit, H., 1997. Coccolithophore fluxes in the Norwegian–Greenland Sea: seasonality and assemblage alterations. Marine Micropaleontology 31, 45–64.

Backman, J., Hermelin, J.O.R., 1986. Morphometry of the Eocene nannofossil *Reticulofenestra umbilicus* and its biochronological consequences. Palaeogeography, Palaeoclimatology, Palaeoecology 57, 103–116.

Bard, E., Arnold, M., Maurice, P., Duprat, J., Moyes, J., Duplessy, J.-C., 1987. Retreat velocity of the North Atlantic polar front during the last deglaciation determined by ^{14}C accelerator mass spectrometry. Nature 328, 791–794.

Bard, E., Fairbanks, R., Arnold, M., Maurice, P., Duprat, J., Moyes, J., Duplessy, J.-C., 1989. Sea-level estimates during the last deglaciation based on $\delta^{18}O$ and accelerator mass spectrometry ^{14}C ages measured in *Globigerina bulloides*. Quaternary Research 31, 381–391.

Bard, E., Rostek, F., Turon, J.-L., Gendreau, S., 2000. Hydrological impact of Heinrich Events in the subtropical Northeast Atlantic. Science 289, 1321–1324.

Bassinot, F., Labeyrie, L., shipboard scientific party, 1996. A coring cruise of the R/V Marion Dufresne in the North Atlantic Ocean and Norwegian Sea. Unpublished report, LSCE. Laboratoire mixte CNRS-CEA, 91198 Gif/Yvette cedex, France.

Bauch, D., Darling, K., Simstich, J., Bauch, H.A., Erlenkeuser, H., Kroon, D., 2003. Palaeoceanographic implications of genetic variation in living North Atlantic *Neogloboquadrina pachyderma*. Nature 424, 299–302.

Baumann, K.-H., 1995. Morphometry of Quaternary *Coccolithus pelagicus* coccoliths from Northern North Atlantic and its paleoceanographical significance. Proceedings 5th INA Conference. Salamanca, Spain, pp. 11–21.

Bond, G., Lotti, R., 1994. Heinrich events: a consequence of sea-level rises? (abstract). EOS Transactions of the American Geophysical Union 75 (16), 54.

Bond, G., Lotti, R., 1995. Icebergs discharge into the North Atlantic on millennial time scales during the last glaciation. Science 267, 1005–1010.

Broecker, W., 1994. Massive icebergs discharge as triggers for global climate change. Nature 372, 421–424.

Broecker, W., Bond, G., Klas, M., Clark, E., McManus, J., 1992. Origin of the northern Atlantic's Heinrich events. Climate Dynamics 6, 265–273.

Cachão, M., Moita, M.T., 2000. *Coccolithus pelagicus*, a productivity proxy related to moderate fronts off Western Iberia. Marine Micropaleontology 39, 131–155.

Calvo, E., Villanueva, J., Grimalt, J.O., Boelaert, A., Labeyrie, L., 2001. New insights into the glacial latitudinal temperature gradients in the North Atlantic. Results from $U^{k'}_{37}$ sea-surface temperatures and terrigenous inputs. Earth and Planetary Science Letters 188, 509–519.

Cayre, O., Lancelot, Y., Vincent, E., Hall, M., 1999. Paleoceanographic reconstructions from planktonic foraminifers off the Iberian margin: temperature, salinity and Heinrich Events. Paleoceanography 14, 384–396.

Colmenero-Hidalgo, E., Flores, J.-A., Sierro, F.J., 2002. Biometry of *Emiliania huxleyi* and its biostratigraphic significance in the Eastern North Atlantic Ocean and Western Mediterranean Sea in the last 20000 years. Marine Micropaleontology 46, 247–263.

de Abreu, L., 2000. High resolution Palaeoceanography off Portugal during the last two Glacial Cycles. Dissertation PhD, University of Cambridge, U. K. 365 pp.

de Abreu, L., Shackleton, N.J., Schönfeld, J., Hall, M., Chapman, M., 2003. Millennial-scale oceanic variability off the Western Iberian margin during the last two glacial periods. Marine Geology 196, 1–20.

Duprat, J., 1983. Les Foraminiféres planctoniques du Quaternaire terminal d'un domaine péricontinental (Golfe de Gascogne, Cotes Ouest-Iberiques, Mer d'Alboran): Ecologie-Biostratigraphy. Bulletin de l'Institut de Géologie du Bassin d'Aquitaine 33, 71–150.

Fasham, M., Platt, T., Irwin, B., Jones, K., 1985. Factors affecting the spatial pattern of the Deep Chlorophyll Maximum in the region of the Azores Front. Progress in Oceanography 14, 129–166.

Fatela, F., 1995. Contribuition des Foraminifères benthiques profonds à la reconstruction des paléoenvironnements du Quaternaire récent de la Marge Ouest Ibérique (Marge Nord Portuguaise et Banc de Galice). These Doctorat, Université de Bordeaux, France. 262 pp.

Fatela, F., Duprat, J., Annick, P., 1994. How Southward Migrated the Polar Front Along the Western Iberian Margin at 17,800 yrs B. P. Gaia-Resumos do 1° Simpósio Sobre a Margem W-Ibérica, vol. 8, pp. 169–173.

Fiúza, A.F.G., Hamann, M., Ambar, I., Díaz del Rio, G., González, N., Cabanas, J.M., 1998. Water masses and their circulation off western Iberia during May 1993. Deep-Sea Research. Part 1. Oceanographic Research Papers 45, 1127–1160.

Geisen, M., Billard, C., Broerse, A., Cros, L., Probert, I., Young, J., 2002. Life-cycle associations involving pairs of holococcolithophorid species: intraspecific variation or cryptic speciation? European Journal of Phycology 37, 531–550.

Gould, W.J., 1985. Physical oceanography of the Azores Front. Progress in Oceanography 14, 167–190.

Heinrich, H., 1988. Origin and consequences of cyclic ice rafting in the Northeast Atlantic Ocean during the past 130,000 yrs. Quaternary Research 29, 142–152.

Hemleben, C., Spindler, M., Anderson, O.R., 1989. Modern Planktonic Foraminifera. Springer-Verlag. 363 pp.

Hurrel, J.M., 1995. Decadal trends in the North Atlantic Oscillation: regional temperatures and precipitation. Science 269, 676–679.

Imbrie, J., Kipp, N.G., 1971. A new micropaleontological method for quantitative paleoclimatology. Application to a late Pleistocene core. In: Terekian, J. (Ed.), The Late Cenozoic Glacial Age. Yale University Press, pp. 71–181.

Johnson, J., Stevens, I., 2000. A fine resolution model of the eastern North Atlantic between the Azores, the Canary Islands and the Gibraltar Strait. Deep-Sea Research. Part 1. Oceanographic Research Papers 47, 875–899.

Jordan, R.W., Cros, L., Young, J.R., 2004. A revised classification scheme for living haptophytes. Micropaleontolology 50 (1), 55–79.

Klein, B., Siedler, G., 1989. On the origin of the Azores Current. Journal of Geophysical Research 94, 6159–6168.

Knappertsbusch, M., 2000. Morphologic evolution of the coccolithophorid *Calcidiscus leptoporus* from the early Miocene to Recent. Journal of Paleontology 74 (4), 712–730.

Lebreiro, S.M., Moreno, J.C., McCave, I.N., Weaver, P.P.E., 1996. Evidence for Heinrich layers off Portugal (Tore Seamount): 39°N, 12°W. Marine Geology 131, 47–56.

Lebreiro, S.M., Moreno, J.C., Abrantes, F.F., Pflaumann, U., 1997. Productivity and paleoceanography implications on the Tore Seamount (Iberian Margin) during the last 225 kyr: foraminiferal evidence. Paleoceanography 12, 718–727.

Martinson, D.O., Pisias, N.G., Hayes, J.D., Imbrie, J., Moore, T.C.J., Shackleton, N.J., 1987. Age dating and the orbital theory of the ice ages: development of a high resolution 0 to 300,000 year chronostratigraphy. Quaternary Research 27, 1–29.

McIntyre, A., Bé, A., 1967. Modern coccolithophores of the Atlantic Ocean: I. Placoliths and cyrtoliths. Deep-Sea Research 14, 561–597.

McManus, J.F., Oppo, D.W., Cullen, J.L., 1999. A 0.5-million-year record of millennial-scale climate variability in the North Atlantic. Science 283, 971–975.

Okada, H., McIntyre, A., 1979. Seasonal distribution of modern Coccolithophores in the Western North Atlantic Ocean. Marine Biology 54, 319–328.

Parente, A., Cachão, M., Baumann, K.-H., de Abreu, L., Ferreira, J., 2004. Morphometry of *Coccolithus pelagicus* s: l. (Coccolithophore, Haptophyta) from offshore Portugal, during the last 200 kyr. Micropaleontology 50 (1), 107–120.

Pflaumann, U., Duprat, J., Pujol, C., Labeyrie, L.D., 1996. SIMMAX: a modern analogue technique to deduce Atlantic sea surface temperatures from planktonic foraminifera in deep-sea sediments. Paleoceanography 11, 15–35.

Roth, P., 1994. Distribution of coccoliths in oceanic sediments. In: Winter, A., Siesser, W. (Eds.), Coccolithophores. Cambridge University Press, Cambridge, pp. 199–218.

Rodó, X., Baert, E., Comin, F.A., 1997. Variations in seasonal rainfall in Southern Europe during the present century: relationships with the North Atlantic Oscillation and the El Niño-Southern Oscillation. Climate Dynamics 13, 275–284.

Ruddiman, W.F., McIntyre, A., 1981. The North Atlantic Ocean during the last deglaciation. Palaeogeography, Palaeoclimatology, Palaeoecology 35, 145–214.

Sáez, A.G., Probert, I., Geisen, M., Quinn, P., Young, J.R., Medlin, L.K., 2003. Pseudo-cryptic speciation in coccolithophores. Proceedings of the National Academy of Sciences of the United States of America 100, 7163–7168.

Samtleben, C., 1980. Die evolution der coccolithophoriden-Gattung *Gephyrocapsa* nach Befunden im Atlantik. Paläontologische Zeitschrift 54, 91–127.

Wei, W., 1992. Biometric study of *Discoaster multiradiatus* and its biochronological utility. Memorie Scienze Geologiche 43, 219–235.

Westbroek, P., de Jong, E.W., van der Wal, P., Borman, A.H., de Vrind, J.P.M., Kok, D., de Bruiin, W.C., Parker, S.B., 1984.

Mechanism of calcification in the marine algae *Emiliania huxleyi*. Philosophical Transactions of the Royal Society of London. Series B, Biological Sciences 304, 435–444.

Winter, A., Jordan, R., Roth, P., 1994. Biogeography of living Coccolithophores in ocean waters. In: Winter, A., Siesser, W. (Eds.), Coccolithophores. Cambridge University Press, Cambridge, pp. 13–37.

Young, J., 1990. Size variation of Neogene *Reticulofenestra* coccoliths from Indian Ocean DSDP cores. Journal of Micropalaeontology 9 (1), 71–86.

Young, J., Davis, S.A., Bown, P.R., Mann, S., 1999. Coccolith ultrastructure and biomineralisation. Journal of Structural Biology 126, 195–215.

Young, J., Henriksen, U., 2003. Biomineralization within vesicles: the calcite of coccoliths. In: Dove, P., Yoreo, J., Weiner, S. (Eds.), Biomineralization, Reviews in Mineralogy and Geochemistry, vol. 54. Mineralogical Society of America, pp. 189–215.

Zazo, C., Goy, J.L., Lario, J., Silva, P.G., 1996. Littoral zone and rapid climatic changes during the last 20,000 years. The Iberia study case. Zeitschrift für Geomorphologie. Supplementband 102, 119–134.